An Arterial Pulse Signal Acquiring Wristwatch with Flexible Tactile Sensing Dense-Array

Yi Sun, Ke Sun, Fang Wang, Yue He, Heng Yang*, Xinxin Li*
State Key Laboratory of Transducer Technology, Shanghai Institute of Microsystem and Information Technology, Chinese Academy of Sciences, Shanghai, China
Email: {sunyi, sunke, f.wang, heyue, h.yang, xxli}@mail.sim.ac.cn

Xikun Zheng, Jingqing Hu
Xin-Huangpu Joint Innovation Institute of Chinese Medicine, Guangzhou, China
Email: 280349199@qq.com, gcp306@126.com

***Abstract*—This study reports a wristwatch to automatically acquire the arterial pulse signal. A two-dimensional flexible tactile sensing dense-array is integrated in the watch. The dense-array consists of 29 × 3 ultra-small pressure sensing chips, enabling high-resolution tactile perception. The arterial pulse signal contains abundant information regarding cardiovascular conditions. Our wristwatch is able to measure the radial arterial pulse in all 8 dimensions: depth, strength, rate, uniformity, fluency, width, stiffness and stability. As far as we know, this is the first wearable system to record the pulse wave not only in time domain but also in cross-section concurrently. With such comprehensive information, physicians have better access to pulse signal in full aspects. The watch has a compact size, low energy consumption and real-time feedback, highlighting its great potential for ambulatory cardiovascular monitoring.**

Keywords—wristwatch, flexible tactile sensing, radial arterial pulse, cardiovascular monitoring

I. Introduction

The arterial pulse wave is a noteworthy physiological signal and has been proved to be an indispensable predictor of manifold cardiovascular diseases. A range of pulse signal acquiring and analyzing systems have been developed in recent decades. Tyan et al. built a two-axis mechanism to detect the radial artery [1]. Jin et al. proposed a pressurization system using airbags and achieved three-region pulse signal measurements after applying different levels of pressure [2]. Chen et al. introduced a system using a micro-electro-mechanical system (MEMS) pressure-sensor array and measured 3D wrist pulse waves to assess pulse width changes before and after exercise [3]. However, the single sensor size is 5.5 × 3.6 mm – almost twice the diameter of the radial artery – which compromises the accuracy of the measurement. Hu et al. applied a 3 × 4 pressure-sensor array with 2.5 × 2.5 mm sensor units to determine the temporal and spatial properties of the arterial pulse [4]. Wang et al. designed a compound pressure signal acquisition system using a sensor array combined with the main sensor and further sub-sensor arrays to solve the problems of sensor positioning and pressure adjustment [5]. These systems utilize single or scattered sensors to locate the artery and sketch time series waveform from those points for medical analysis.

Nevertheless, the most incisive problem in previous systems lies in the sensors employed are so large that they are only able to record the isolated waveform in time domain, but more informative envelope shapes in cross-section are thus missing. Equipped with the flexible tactile sensing dense-array, our newly-developed wristwatch aims to acquire the arterial pulse signal in both radial and axial directions, enabling physicians access pulse information in full aspects.

II. Hardware Design

A. Flexible Tactile Sensing Dense-Array

In order to achieve high-resolution tactile perception, a sort of mini-size absolute pressure sensors previously designed by our research group are employed in the dense-array. 29 such micro pressure sensors are packaged on a flexible printed circuit (FPC) board in a straight line to form a unidimensional tactile sensing dense-array with a span of 16.80 mm, easily achieving full coverage of the radial artery region in the wrist. The dense-array has a pitch of 0.60 mm, already reaching the human fingertip touch resolution, which allows sensitive perception of subtle changes in pressure distribution.

B. Arterial Pulse Signal Acquiring Wristwatch

User wears the watch and let the 3 sub-arrays cover the radial artery perpendicularly. First, the arrays are pressed into the skin by 3 motors and deforms the artery to the most. Then

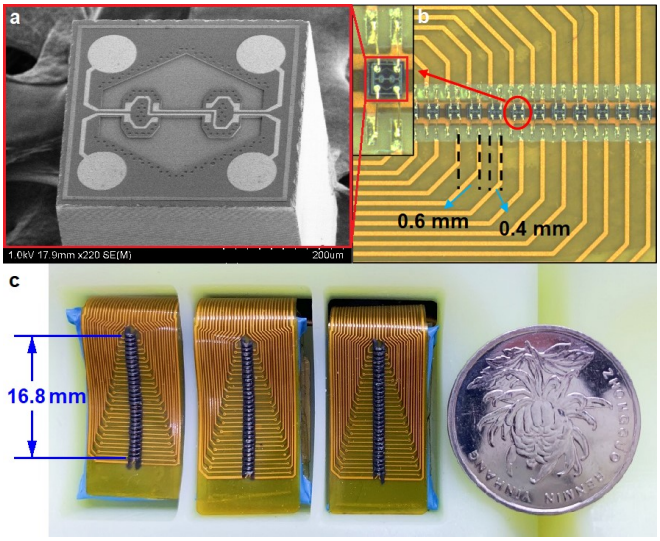

Fig. 1. The wristwatch with flexible tactile sensing dense-array. **a** The scanning electron microscope (SEM) image of one MEMS pressure sensing chip. **b** The two-dimensional array involves 29 × 3 ultrasmall pressure sensors (0.4 mm × 0.4 mm each) with a pitch of 0.60 mm, allowing high resolution acquisition of tactile information. **c** The array has a sensing span of 16.80 mm.

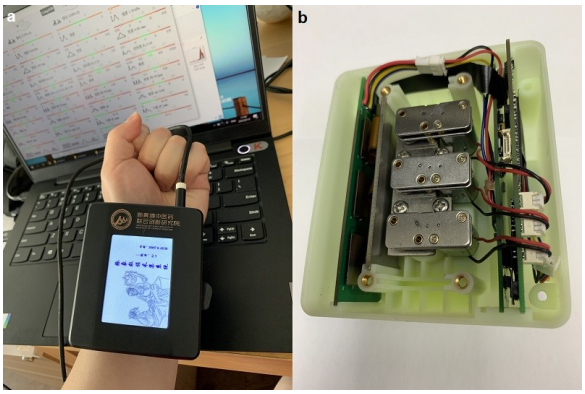

Fig. 2. **a** Being worn in the wrist, the watch measures all 8 attributes of arterial pulse. The results are on display on both watch and server. **b** Three motors press the three sub-arrays into the skin separately to sense the change in pressure distribution. Subsequently, the attributes "depth" and "stiffness" will be calculated according to these changes.

the motors gradually retreat, from the deepest to the shallowest at 6 depths. While the flattened vessel returns to normal, the arrays sense the tactile mappings under the diminishing 6 stresses. The sampling rate is set to 400 Hz, the motors stop at each of the 6 depths for 5 sec. This dynamic operation is to determine the pulse depth and stiffness.

III. Algorithms of the Eight Attributes

With the tactile mappings sampled under 6 external stresses, all 8 pulse attributes in both time domain and cross-section are calculated successively.

A. Pre-processing

(1) Sensitivity Calibration:

The pressure sensors are MEMS chips and have inherent distinctions inevitably. Before being packaged in the wristwatch, all 87 sensors were sealed in a pressure chamber, so that their actual outputs under identical air pressures were tested. Then, 2 exclusive calibration parameters for each sensor are measured accordingly. With these parameters, all sensor's readings are therefore consistent. In this procedure the unit of sensor's output is also converted from mV into kPa.

(2) Low Pass Filter:

The raw data is first processed by a low pass filter through which the jitters caused by noise with high frequency are eliminated. Here a moving average filter with a buffer size of sampling rate / 26.6667 = 15 sampling points is utilized.

(3) Removing the Direct Current (DC) Component

Within each sample (5 sec), the minimum of a certain sensor's output is regarded as the DC component of that channel. The value of the DC component is also referred to as the static pressure and is supposed to be subtracted from the original values. The static pressure may also serve as an indicator in the initial self-test for a sensor. If a sensor output a minus static pressure value, that sensor is more likely to be broken and the data from that channel is treated unreliable and will be interpolated by the mean values of 2 adjacent channels.

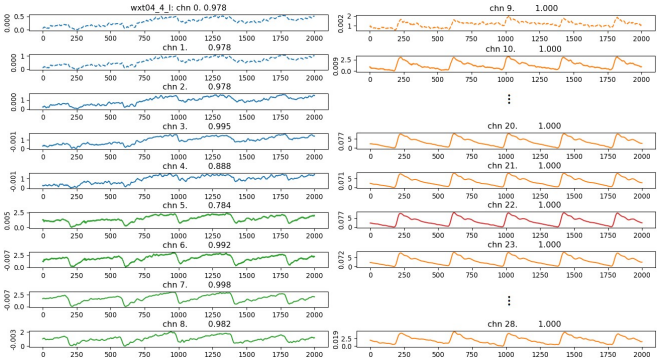

Fig. 3. The signals sampled by the 29 sensors in a sub-array. Due to the space limitation, some channels sharing similar waveforms are omitted. The curves in orange are valid signals from which the pulse waveform is clear and distinguishable. They are sampled by sensors closely attached to the radial artery. Among them the 22nd channel (in red) records the most intense signal and is therefore taken as the main channel. The curves in green are generated by sensors above the radius on one side of the radial artery. Because the radius is hard, the pulse wave would rebound off the bone and be recorded in an inverse form. These channels are labeled as inverse channels. The channels in blue are invalid channels from which no meaningful signal is found. The curves in dotted line mean the sensors are broken. They are interpolated by adjacent channels. As frequent experiments, damage to individual sensors is inevitable. However, it is also not necessary to replace the broken ones immediately, as long as the distortion caused by interpolation is still tolerable.

(4) Identification among Valid / Invalid / Inverse Channels

The diameter of the radial artery is 2 – 3 cm, while the sensing span of our array reaches 16.80 cm. Being worn in the wrist, the watch has little difficulty in covering the pulsatile vessel, but positioning the activated area in the array proved to be a vexing challenge, which involves automatically and precisely identifying the valid / invalid / inverse channels.

The algorithm for channel identification:

Step 1: determine the main channel.

Step 1.1, aggregate the values in each channel to find local peak channels (LPCs). The LPCs are defined as the channels with larger aggregate values than their 2 adjacent channels.

Step 1.2, calculate the Wave Indicator (WI) for each LPC. First, the differential sequence of the signal is computed. POS is the mean value of all positive numbers in the differential sequence; while NEG is the mean value of all negative numbers in the differential sequence. As a result, WI is defined as POS + NEG. The LPC with the largest and positive WI is designated as the main channel (e.g. Fig. 3, channel 22, in red).

Step 1.3, if none of LPC's WI was larger than 0, no meaningful signal is found. The whole sample is invalid!

Step 2: compare other channels with the main channel.

Step 2.1, calculate the amplitude spectrum of each channel. Step 2.2, check the "consistency" between their amplitude spectrums and the main channel's. The standards of consistency lie in:

s.t. 1: the highest spectral line shares the same x-coordinate with the main channel's highest spectral line. That means its

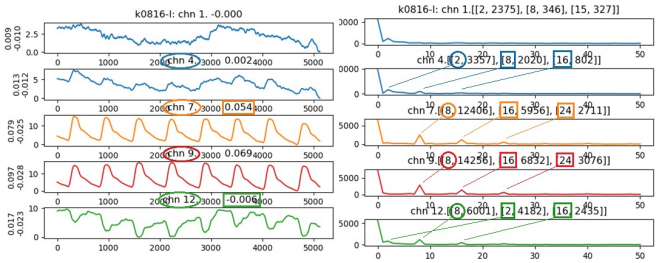

Fig. 4. An instance of channel identification with amplitude spectrum. The first 3 highest spectral lines of the main channel (channel 9, red) locate at frequencies 8, 16 and 24. Channel 7 (orange)'s first 3 highest: 8, 16, 24, exactly the same, so its amplitude spectrum is consistent with that of the main channel. Besides, the WI of Channel 7 is 0.054 > 0. So, Channel 7 is identified as a valid channel. Channel 12 (green)'s first 3 highest: 8, 2, 16. The highest are both at 8. The 2nds and 3rds share the common 16, meeting s.t. 2. So, its amplitude spectrum is also consistent with that of the main channel. But Channel 12's WI is -0.006 < 0. Accordingly, it is categorized as an inverse channel. Channel 4 (blue): 2, 8, 16, the highest are not the same with the main channel's. Although it has common x-coordinates at 2nd or 3rd, only s.t. 2 is met, invalid.

most powerful component must have the same frequency with that of the main channel's most powerful component.

s.t. 2: in terms of the 2nd and 3rd highest spectral lines, they must have at least 1 common x-coordinates with those of the main channel.

These 2 standards are exemplified in the cases of Fig. 4.

Step 3: identify other valid channels and inverse channels.

Step 3.1, if the channel's amplitude spectrum was not consistent with that of the main channel, the channel will be categorized as an invalid channel (Fig. 3, channels 0 – 4, blue).

Step 3.2, if the channel's amplitude spectrum was consistent with that of the main channel:

Step 3.2.1, if the channel's WI is larger than 0, the channel would be identified as a valid channel (Fig. 3, channels 9 – 21, channels 23 – 28, orange).

Step 3.2.2, if the channel's WI is negative, the channel is classified as an inverse channel (Fig. 3, channels 5 – 8, green).

B. Pulse Depth

The determination for pulse depth is the prerequisite to measure other 7 attributes. As shown in Fig. 5 (concerning only main channel), waveform is detected at every depths. In most cases, not all of these waves will be analyzed. Only if the signal's average peak – trough amplitude is the largest, it would be selected for further time domain analysis (strength, rate, uniformity, fluency), and that depth would be taken as the depth of the pulse.

C. Pulse Strength

The 4 attributes: strength, rate, uniformity, and fluency are calculated based solely on the signal sampled in the main channel at the "right" depth interpreted in the section *B*. The pulse strength is defined as the average peak – trough amplitude of all cycles. According to clinical statistics, 4 thresholds: 2, 5, 15, 20 kPa are set to divide the pulse strength into 5 levels:

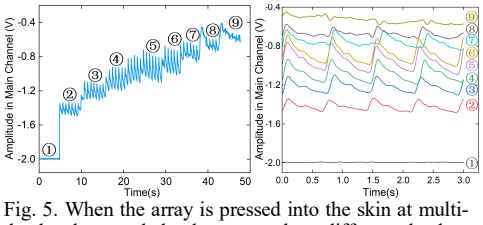

Fig. 5. When the array is pressed into the skin at multi-depths, the sampled pulse waves show different absolute amplitudes. It is not that the bigger the force applied, the greater the amplitude. At the 5th depth, the signal has the most intense waveform. As a result, that depth is selected as the "pulse depth". Here, for better display, the depth is divided into 9 layers. In practice, it is rather time-consuming (takes nearly 50 sec), so we reduce it to 6 depths in our wristwatch.

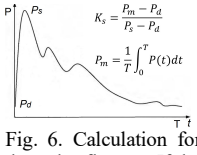

Fig. 6. Calculation for the pulse fluency. If the pulse is fluent, the arterial wall shows good elasticity, that means the signal takes sooner to drop after reaching its peak. The shorter the time the pressure remains at a high level, the lower *Ks* a subject has, the healthier the subject.

extremely weak: (0, 2); weak : [2, 5); normal: [5, 15];
intense: (15, 20]; extremely intense: (20, +∞).

D. Pulse Rate

The basic function that no sphygmometer lacks. It is calculated as the quotient of the number of cycles and the duration of all the cycles (in min). 6 thresholds: 30, 50, 60, 90, 120, 220 bpm divide the pulse rate into 5 levels:

extremely slow: [30, 50); slow: [50, 60);
normal: [60, 90]; fast: (90, 120]; extremely fast: (120, 220].

E. Pulse Uniformity

This attribute is measured by Coefficient of Variation (CV):

$$\mathrm{CV} = \sigma_{\mathrm{IBI}} / \mu_{\mathrm{IBI}} \qquad (1)$$

, where IBI stands for Inter-Beat Interval (in ms); σ and μ denote the calculation for standard deviation and mean value. Pulse uniformity has a strong relation with sinus rhythm and may serve as an independent indicator of arrhythmia. The larger the uniformity, the bigger the risk. 2 thresholds: 0.1, 0.12 divide the uniformity into 3 levels:

uniform: [0, 0.1]; nonuniform: (0.1, 0.12];
extremely nonuniform: (0.12, +∞).

F. Pulse Fluency

This attribute reflects vascular elasticity and compliance. The fluency *Ks* is calculated as Fig. 6, P_s and P_d represent the systolic and diastolic pressures, respectively; while P_m denotes the average pressure. 4 thresholds: 0.25, 0.35, 0.4, 0.5 divide the fluency into 5 levels:

extremely fluent: (0, 0.25); normal: [0.25, 0.35];
slightly dysfluent: (0.35, 0.4]; dysfluent: (0.4, 0.5];
extremely dysfluent: (0.5, 1).

G. Pulse Width

If the 4 attributes about the time domain could also be measured by traditional sphygmometers with single or scattered sensors, acquiring the next 3 attributes regarding pulse shapes in cross-section proved incapable for them. In this study the dense-array's activated width is found to be exactly the static pulse width. However, more often than not, physicians care more about the dynamic pulse width (Fig. 7):

Ds = Area of the shadow / Area under the blue curve (2)

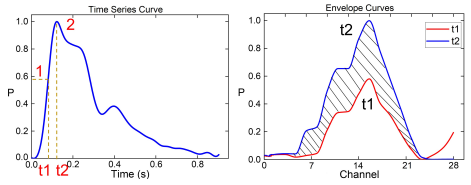

Fig. 7. Dynamic pulse width (*Ds*) estimation with envelope curves. *Ds* is a factor about variability. The more significant the pulse expansion, the larger the *Ds*. More details about are found in our published work [6].

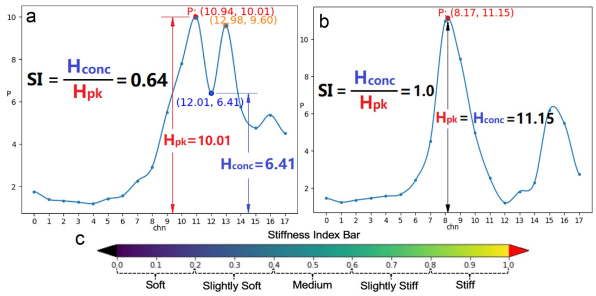

Fig. 8. Calculation of stiffness index (SI) with envelope curves. **a** Definition of SI. **b** A case of arteriosclerosis in clinical diagnosis (SI = 1). **c** Stiffness Index Bar (The closer the SI gets to 1, the stiffer it is; the closer to 0, the softer) [7].

H. Pulse Stiffness

Pulse stiffness is a property about the degree of arterial wall degeneration or fibrosis. As people age, their arteries will inevitably become increasingly stiffer, due to the loss of elastin in their arterial walls. Some lesions like atherosclerosis or arteriosclerosis will also accelerate the degeneration in arterial wall to make it thicker and stiffer. We developed a solution to estimate the stiffness and grade it (Fig. 8) [7].

I. Pulse Stability

Sometimes when people are suffering pain or fever, their heart rates will rise. A surge in blood flow may cause temporary throb of the vessel and this unsteadiness would also be detected by our wristwatch. We refer to it as "horizontal instability". As shown in Fig. 10, the barycenter of the cross-section varies from cycle to cycle. The pulse instability is measured by the standard deviation of the barycenter's *x*-coordinate for at least 6 successive cycles. 2 thresholds: 0.11 and 0.2 divide the instability into 3 levels:

stable: [0, 0.11];
instable: (0.11, 0.2]; extremely instable: (0.2, +∞).

Fig. 9. The screenshot of the user interface. All 8 pulse attributes are marked on their respective scales in real time. Not only the measurement values but their intervals for cardiovascular risk stratification are on display. Click the 4 buttons on the left to open (1) time series figures of all channels, (2) detailed time series figure of the main channel, (3) envelope curves of all cycles, and (4) 3D GIF of pulse envelope surface.

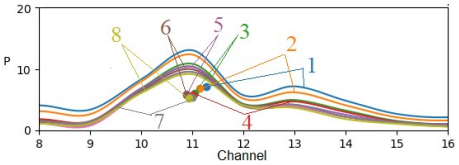

Fig. 10. If the heart rate or blood pressure was instable, the artery throbs irregularly. When it comes to the pulse's cross-section, the barycenter vibrates as well. This instability is mainly found in the horizontal direction. This figure shows the envelope curves for 8 successive cycles in this case, from which the barycenter's lateral drift is distinctly revealed.

IV. Evaluatione and Conclusion

The comparison among our wristwatch and the previous systems is listed in Table I. Our solution possesses unique advantages over them.

TABLE I. Comparison among Available Systems

System	Tyan[1]	Jin[2]	Chen[3]	Hu[4]	Wang[5]	Ours
Sensors Num	1	3	3×4	3×4	12×3	29×3
Sensor Size (mm)	Φ12	5.6^2	5.5×3.6	2.5^2	0.8×8	0.4^2
Flexible	No	No	Yes	No	No	Yes
Wearable	No	No	No	No	No	Yes
Pulse Positioning	No	No	No	No	Yes	Yes
Features in Cross-section	No	No	Yes	No	Yes	Yes

A wristwatch equipped with flexible tactile sensing array to measure arterial pulse signal is proposed in this paper. Our dense array can not only record the waveform in time series but acquire envelope information in cross-section, which is of great superiority in thorough cardiovascular monitoring.

Acknowledgment

This work is supported by the Innovation Team and Talents Cultivation Program of National Administration of Traditional Chinese Medicine (ZYYCXTD-D-202003) and Guangdong Provincial Key Field R&D Plan Project (2020B1111120004).

References

[1] C. C. Tyan, S. H. Liu, J. Y. Chen, J. J. Chen, and W. M. Liang, "A novel noninvasive measurement technique for analyzing the pressure pulse waveform of the radial artery," *IEEE Trans. Biomed. Eng.*, vol. 55, no. 1, pp. 288–297, 2008.

[2] C. Jin, C. Xia, S. Zhang, L. Wang, Y. Wang, and H. Yan, "A wearable combined wrist pulse measurement system using airbags for pressurization," *Sensors* (*Switzerland*), vol. 19, no. 2, 2019.

[3] C. Chen, Z. Li, Y. Zhang, S. Zhang, J. Hou, H. Zhang, "A 3D wrist pulse signal acquisition system for width information of pulse wave", Sensors (*Switzerland*) 2020, 20, 11.

[4] C. Hu, Y. Chung, C. Yeh, C. Luo, "Temporal and spatial properties of arterial pulsation measurement using pressure sensor array", *Evidence-based Complement. Altern. Med.* 2012.

[5] P. Wang, W. Zuo, and D. Zhang, "A compound pressure signal acquisition system for multichannel wrist pulse signal analysis", *IEEE Trans. Instrum. Meas*. vol. 63, no. 6, pp. 1556–1565, 2014.

[6] J. Chen, Y. Sun, K. Sun, H. Yang, X. Li, "Finger-worn Dense Pressure-sensor Array for Arterial Pulse Acquisition", in *21st International Conference on Solid-State Sensors, Actuators and Microsystems* (*Transducers*), Orlando, FL, USA, June 20-24, 2021, pp. 1468-1471.

[7] F. Wang, H. Yang, K. Sun, Y. Sun, X. Li, "Non-invasive instant measurement of arterial stiffness based on high-density flexible sensor array", in *36th IEEE International Conf on Micro Electro Mechanical Systems* (*MEMS*), Munich, Germany, Jan 15-19, 2023, pp. 351-354.